Renewable Energy 74 (2015) 37–48

Contents lists available at ScienceDirect

Renewable Energy

journal homepage: www.elsevier.com/locate/renene

Designing multi-well layout for enhanced geothermal system to better exploit hot dry rock geothermal energy

Jiliang Chen, Fangming Jiang*

Laboratory of Advanced Energy Systems, CAS Key Laboratory of Renewable Energy, Guangzhou Institute of Energy Conversion, Chinese Academy of Sciences (CAS), Guangzhou 510640, China

ARTICLE INFO

Article history:
Received 6 January 2014
Accepted 28 July 2014
Available online 20 August 2014

Keywords:
Hot dry rock
Enhanced geothermal system
Well layout
System optimization design
Numerical model

ABSTRACT

Heat extraction mode, e.g. well layout or arrangement of wells, of enhanced or engineered geothermal system (EGS) is crucial to its performance and directly affects its commercial viability. Assuming the subsurface target hot dry rock (HDR) has been well-fractured and the created heat reservoir can be treated as a homogeneous porous medium, we numerically simulate the long-term heat extraction process of EGSs of various well layouts, including the standard doublet well layout, two triplet well layouts, and a quintuplet well layout. The simulation results enable a detailed analysis on the effects of well layout on EGS heat extraction performance. We find simply deploying more production wells does not necessarily improve the EGS heat extraction performance; an EGS with triplet well layout can perform better than an EGS with a quintuplet well layout or worse than an EGS with the standard doublet well layout. One more finding is an EGS with the injection well positioned close to the edge of the reservoir gets more thermal compensation from the un-fractured rocks surrounding the reservoir during heat extraction. Further, we deduce an optimized EGS well layout must ensure enough long major flow path and less preferential flow in the reservoir, and the injection well is located close to the edge of the reservoir. We then design a quartuplet well layout accordingly. Results from an additional simulation with respect to the quartuplet well EGS indicate its enhanced heat extraction performance, corroborating the success of design. Last, we discuss about the hot dry rock (HDR) heat recovery factor based on numerous simulated cases and estimate the amount of HDR geothermal resource that can be converted into electricity by EGS.

1. Introduction

There exists enormous heat in hot dry rocks (HDRs) beneath the planet. It was reported that the total HDR heat within subsurface 3–10 km depths of the United States (US) territory is more than 14×10^6 EJ [1]. A recent assessment conveyed that the storage of HDR heat within subsurface 3–10 km depths in China mainland is about 25×10^6 EJ [2]. Both are huge amounts compared with the total energy consumption in US or China, which is only about 100 EJ annually [1,2]. The HDR heat represents a large, indigenous energy resource that has the potential to provide base-load electric power with no or little environmental footprint [3]. Exploiting heat from HDR may be an important strategy to meet the fast-growing energy demand.

Research and development on the extraction and utilization of HDR heat started a few decades ago [1], dated back to the early 1970s when the concept of enhanced or engineered geothermal system (EGS) was first proposed by a group of US scientists. In the construction of EGS, a well is drilled to the target HDR and stimulation treatments are then performed to engineer the target HDR. After an artificial reservoir of adequate flow conductivity and sufficient heat exchange area is created, cold fluids are injected to flow through the reservoir. Heat stored in the HDR is transferred to the injected fluids and the heat-carrying hot fluids are harvested at the production well/wells. The outflow hot fluids are for earth-surface power-generation and/or direct heat utilizations. The exhaust fluids may be re-injected into the reservoir to form a circulation loop.

EGS has been widely envisaged as the major development direction of future geothermal energy utilization. Numerous projects [5–9] aimed at developing techniques for the creation of EGS pilot plants, have been and are still being conducted around the world.

* Corresponding author. Tel.: +86 20 87057656.
E-mail addresses: fm_jiang2013@yahoo.com, fm_jiang2000@yahoo.com (F. Jiang).

http://dx.doi.org/10.1016/j.renene.2014.07.056
0960-1481/

However, there is no an EGS plant that has been really commercialized to date. Designing advanced heat extraction modes (e.g. well layout or arrangement of wells) to efficiently mine heat from subsurface HDRs may improve the performance–cost ratio of EGS and accelerate its commercialization.

The procedures for constructing an EGS include geological investigation for site-picking, well-drilling, reservoir stimulation, construction of fluid-circulation system, construction of earth-surface power station, and installation of power transmission lines. Well-drilling is a requisite and the most costly procedure, as evident in many geothermal projects [1]. It was reported that the cost of well-drilling could amount to 50%–60% or more of the total capital investment [10,11]. The well-drilling technology is relatively mature as it has been developed and applied in the oil and gas industry for decades [12,13]. However, geothermal drilling, especially for applications in EGS, is often far more difficult than in the oil and gas operations as the HDR is usually harder and of higher temperature, and the fluids may be corrosive to the drill bit as well [10–14]. New technologies of borehole drilling are critically needed in the development of commercially viable EGS. A proper design of well layout may reduce technical risks at well-drilling and bring positive effects on the economic performance of EGS.

The single well productivity is a key factor dictating the commercial viability of EGS. An outflow of 80 kg/s flow rate with fluid temperature at 423.15 K or higher is the target for an EGS to achieve the goal of commercial operation [4]. No field tests have realized this target so far. The EGS project at Soultz has reported a maximum well productivity of about 26 kg/s [8]. To achieve sufficiently high well productivity remains to be a big challenge to the commercialization of EGS. The low circulation flow rate was mainly caused by the low permeability of the stimulated reservoir and the poor inter-well connectivity [15,16]. The multi-well strategy can add fracturing implementation loci, which is helpful in stimulating more fissures and somewhat homogenizes the distribution of permeability and porosity in the reservoir. Arranging more wells can generally shorten the well distance and can enhance the subsurface inter-well connectivity, facilitating the fluid circulation and at the same time reducing the possibility of fluid loss. Given the current rock fracturing technologies, the multi-well strategy may be one of the few effective methods to improve the well productivity. However, as aforementioned, the well-drilling is very time-consuming and costly. An optimal design to the well layout is absolutely needed before commencing practical well-drilling.

During the operation of an EGS, there undergoes a coupled thermal-hydraulic–mechanical–chemical (THMC) process in the subsurface fractured rock mass [17,18]. Nevertheless, the fluid flow and heat transfer (TH) process occurs in the subsurface region(s) of EGS play a pivotal role in the involved heat extraction process [19–21]. We have recently developed a 3D transient model, which is capable of modeling long-term heat extraction processes of EGSs [22,23]. This model focuses on the complete subsurface heat exchange (i.e. TH) process and safely neglects the chemical and mechanical (CM) actions between the rock and fluid.

The purpose of the present work is to scrutinize the effects of well layout on EGS heat extraction performance. We model the heat extraction processes of EGSs with various well layouts with the previous model [22,23]. The standard doublet (one injection well, one production well), two triplets (one injection well, two production wells) and a quintuplet (one injection well, four production wells) well EGSs are considered. Design and optimization of EGS well layout will be discussed accordingly. Moreover, we assess the recoverable HDR heat resource according to the overall heat extraction factor derived from a large quantity of model results.

2. Methodology

2.1. Model equations and concepts

We have previously reported a three-dimensional numerical model for the simulation of EGS long-term heat extraction processes [22,23]. In this model, the heat reservoir is treated as an equivalent porous medium characterized by some macroscopic properties (e.g. porosity and permeability) without considering any detailed information on fracture morphology and location. During the operation of EGS, the fluid injection temperature ranges from 300 to 350 K, evident temperature differences exist between the rock and heat transmission fluid in some portion or even most of the reservoir. The model considers local thermal non-equilibrium between the solid rock matrix and fluid flowing in the fractured rock, and employs two energy conservation equations to describe the temperature evolution of the rock matrix and of the heat transmission fluid in the fractures, respectively, enabling the modeling and analyses of local convective heat exchange in the reservoir. Another salient feature of this model is its capability of simulating the complete subsurface heat extraction process in EGS. The model treats the EGS subsurface multiple domains as a single-domain of three subregions associated with different sets of geophysical properties. Sub-region 1 represents the porous heat reservoir of finite porosity and permeability; sub-region 2 the impermeable solid rocks enclosing the heat reservoir; sub-region 3 the open-channel injection and production wells of unity porosity and infinite permeability. This single-domain treatment circumvents typical difficulties about matching boundary conditions between sub-domains in traditional multi-domain approaches and facilitates numerical implementation and simulation of the complete subsurface heat exchange process. The governing equations of this model are presented as follows.

Mass continuity equation:

$$\frac{\partial(\varepsilon\rho)}{\partial t} + \nabla\cdot(\rho\mathbf{u}) = 0 \tag{1}$$

Momentum conservation equation:

$$\frac{\partial\left(\rho\frac{\mathbf{u}}{\varepsilon}\right)}{\partial t} + \nabla\left(\rho\frac{\mathbf{u}}{\varepsilon}\cdot\frac{\mathbf{u}}{\varepsilon}\right) = -\nabla P + \nabla\cdot\mu^{\mathrm{eqv}}\nabla\frac{\mathbf{u}}{\varepsilon} - \frac{\mu}{K}\mathbf{u} + \rho\mathbf{g} \tag{2}$$

Energy conservation equation for the heat transmission fluid flowing in the fractures:

$$\frac{\partial\left[\varepsilon(\rho c_{\mathrm{p}})_{\mathrm{f}}T_{\mathrm{f}}\right]}{\partial t} + \mathbf{u}\cdot\nabla\left[(\rho c_{\mathrm{p}})_{\mathrm{f}}T_{\mathrm{f}}\right] = \nabla\cdot\left(k_{\mathrm{f}}^{\mathrm{eff}}\nabla T_{\mathrm{f}}\right) + ha(T_{\mathrm{s}} - T_{\mathrm{f}}) \tag{3}$$

Energy conservation equation for heat transport in the rock matrix of the heat reservoir or in the surrounding impermeable rocks:

$$\frac{\partial\left[(1-\varepsilon)(\rho c_{\mathrm{p}})_{\mathrm{s}}T_{\mathrm{s}}\right]}{\partial t} = \nabla\cdot\left(k_{\mathrm{s}}^{\mathrm{eff}}\nabla T_{\mathrm{s}}\right) - ha(T_{\mathrm{s}} - T_{\mathrm{f}}) \tag{4}$$

The application of the full-form Navier–Stokes momentum equation, Eq. (2), enables a general treatment to the fluid flow in open-channel injection and production wells and in the porous heat reservoir. Two energy equations, Eqs. (3) and (4) are used. One is for the heat conduction in HDR (or rock matrix); the other for the heat convection and advection in the fluid. In each of the energy equations there is a term $\pm\, ha(T_{\mathrm{s}} - T_{\mathrm{f}})$ introduced to describe the heat exchange between the solid rock matrix and fluid flowing in the fractures of the reservoir. The effective heat conductivities

k^{eff}–s in Eqs. (3) and (4) are determined in terms of the Bruggeman theorem with a correction factor of 1.5, i.e. $k_s^{eff} = k_s(1-\varepsilon)^{1.5}$and $k_f^{eff} = k_f\varepsilon^{1.5}$. More descriptions about this model, such as mathematical-physical assumptions, have already been detailed in Refs. [22,23] and are thus not repeated herein.

To facilitate analyses and discussion, we define six parameters relevant to the EGS heat extraction process.

1) Production temperature $T_{f,out}(t)$: the fluid temperature at the outlet of the production well.
2) EGS abandonment temperature $T_{f,a}$: the outflow fluid temperature being 10 K lower than the maximum production temperature, different from its general definition that is referred to the average rock temperature in the reservoir being 10 K lower than its initial value [24–26]. For example, if the maximum production temperature is 460 K, the EGS abandonment temperature should be 450 K, allowing 10 K temperature drop of the outflow fluid. We put forth this definition of EGS abandonment temperature mainly due to the reason that the performance of relevant equipments is affected directly by the production temperature [27], instead of the rock temperature in the reservoir.
3) EGS service-time or lifetime τ: the time-duration for an EGS being operated until the production temperature $T_{f,out}(t)$ declines down to the EGS abandonment temperature $T_{f,a}$.
4) Local heat extraction ratio $\gamma_L(t)$: the extracted heat divided by the stored heat, locally. As the heat capacity and density of the rock are assumed constant, the definition of γ_L can be expressed as

$$\gamma_L(t) = \frac{T_{s,i} - T_s(t)}{T_s(t) - T_o} \tag{5}$$

where $T_{s,i}$, $T_s(t)$ and T_o represent the initial local rock temperature, the local rock temperature at time instant t, and the ground surface temperature, respectively.

5) Overall heat extraction ratio $\gamma(t)$: the volumetric average heat extraction ratio in the reservoir, that is,

$$\gamma(t) = \frac{\int_{V_R} \gamma_L(t)\mathrm{d}v}{V_R} \tag{6}$$

where V_R represents the reservoir volume.

6) Proportion of thermal compensation from rocks enclosing the reservoir, $\beta(t)$: the heat extracted from the surrounding impermeable hot rocks divided by the accumulative heat extraction amount of the fluid, that is

$$\beta(t) = \frac{\int_{V_s} \left[T_{s,i} - T_s(t)\right](\rho c_p)_s \mathrm{d}V}{\int_0^t Q\left[T_{f,out}(t') - T_{f,in}\right](\rho c_p)_f \mathrm{d}t'} \tag{7}$$

where V_S is the volume of the rocks enclosing the reservoir and Q the volumetric flow rate of the heat transmission fluid. V_S is physically infinite, but practically only the rocks that are close enough to the heat reservoir will have detectable contribution to the heating of the heat transmission fluid.

2.2. Model parameters

2.2.1. Reservoir permeability and porosity

Reservoir permeability and porosity may be the two most important parameters dominating EGS heat extraction process. They dictate the flow distribution and the flow resistance (i.e. the needed external pump work) and thereby directly affect the EGS performance, including the heat extraction performance, lifetime, and economic performance etc. Many factors, such as the rock local stress state, in-situ natural fractures, fluid injection pressure, and rock/fluid chemical composition, may play important roles in the engineering of EGS reservoir [28–30]. The rock temperature evolution during the operation of EGS can also greatly change the reservoir permeability and/or porosity as the hot rock contracts in response to the injected cold fluid [31–33]. Limited by the current technologies, it is almost impossible to obtain the detailed local distributive information of the permeability and porosity in the reservoir. Literature works suggested overall reservoir permeability and porosity values, while both are very divergent data (even for the same EGS test/demonstration field) ranging from 10^{-4} [15,21] to 10^{-2} [17,18,34] for the reservoir porosity and 10^{-8} [35] to 10^{-18} m^2 [19,36] for the reservoir permeability. In the present work, we assume that the EGS reservoir has been homogeneously fractured, being of constant and uniform porosity and permeability, which are 0.01 and 10^{-14} m^2, respectively.

2.2.2. Thermophysical properties

Though the suggestion of using supercritical CO_2 as EGS heat transmission fluid has been proposed for years [37], liquid water is still the most common heat transmission medium used in the to-be-developed or in-operation EGS plants. The present work takes liquid water as the heat transmission fluid and assumes no phase change occurring during the subsurface heat extraction process. Thermophysical properties of the fluid and rock are constant, not changing with temperature and/or pressure, as listed in Table 1.

Local geothermal gradient is an important factor considered during EGS site-picking. The geothermal gradient of the selected EGS site is usually higher than the average value to avoid too deep well-drilling. The present work assumes a constant geothermal gradient, 4 K/100 m, which means the rock temperature at subsurface 4000 m depth is 460 K, given a 300 K ground temperature.

2.2.3. Geometrical conditions

The volume of the created reservoir determines the total thermal energy that is directly exposed to the heat transmission fluid. It is an important factor affecting the commercial viability of EGS. Though no concrete proofs can explicitly show the geometrical configuration of the reservoir, micro-seismicity measurements are able to reveal its approximate volume [38–40]. Rock-fracturing technologies have already demonstrated its capability of creating up to 3 km^3 reservoirs [1]. The shape of artificial reservoirs is highly irregular and very hard to describe; the boundary between the reservoir and surrounding

Table 1
Thermophysical properties of fluid and rock.

	Thermal capacity (J/kg/K)	Thermal conductivity (W/m/K)	Density (kg/m^3)	Viscosity (kg/m/s)
Fluid	4200	0.6	1000	0.001
Rock	1000	2.1	2650	N/A

un-fractured rocks is hard to define because of the spatially gradual change of fracture network caused by, for instance, the hydrothermal alteration effects on the rock permeability and porosity [38–41]. The reservoir considered in this particular work is a 500 × 500 × 500 m cubic volume, centered at subsurface 4000 m depth. From the assumed 4 K/100 m geothermal gradient and 300 K ground temperature, it is easy to calculate the average temperature in the reservoir, 460 K. This geothermal resource can meet the general temperature demand of an ordinary geothermal power plant.

The geometry, including geometrical dimensions of the standard doublet (one injection well and one production well) well EGS is displayed in Fig. 1. The distance from the well center to the nearby reservoir boundary is 50 m. The simulated domain is a 2000 × 6000 × 2000 m volume. The injection and production wells are both 0.2 × 0.2 m square-shaped on the *xy*-plane. In Fig. 1 also presented is the numerical mesh system. Structural hexahedral meshes are used to discretize the whole domain and the meshing process is elaborately controlled to ensure sufficient fine meshes in the injection and production wells and in the reservoir. Totally, there are about 270,000 numerical elements. Grid-independence tests have been conducted to guarantee the present mesh system gives solutions of satisfying accuracy.

We perceive the well layout has profound effects on the EGS performance [22] thereby design four well layouts, as sketched in Fig. 2, for a thorough study to the relevant effects. Besides the standard doublet well layout, we have designed two triplet well EGSs with one injection well and two production wells, and a quintuplet well EGS with one injection well and four surrounding production wells. Particularly for the triplet well EGSs, in terms of the relative positions of the three wells, there are two well layouts considered. One has a triangular arrangement about the three wells (referred as triplet-triangle hereinafter), as shown in Fig. 2c; the other has the three wells aligned along a straightline (referred as triplet-straightline hereinafter), as shown in Fig. 2b.

2.2.4. Other model parameters

We consider all the four cases, as tabulated in Table 2, have the same fluid injection rate, 50 kg/s, while the single-well fluid productivity varies from 12.5 to 50 kg/s owing to different number of production well(s). Cases differ from each other due to the reservoir well layout and/or the single-well productivity. The parameters, *h* and *a*, reflect actually the constitutive condition for heat exchange between the fluid flowing in the fractures and the rock matrix in the reservoir. We consider the product of *h* and *a* as a single parameter and specify it to be 1.0 W/m^2/K for all the cases. Initially, the injection and production wells are full of water of temperature 300 K; the temperature of water in the fractures of the reservoir is equal to the local rock matrix temperature. The inflow water temperature is fixed at 343.15 K. For the fluid flow, the inlet boundary condition is fixed mass flow rate and the outflow boundary condition fixed fluid pressure.

3. Results and analyses

We numerically solved the group of governing equations, Eqs. (1)–(4), for all the four cases. The solution strategies have already been detailed in Refs. [22,23] and are thus not repeated here.

3.1. Heat extraction of doublet EGS

Preferential or short-circuit flow in reservoir is a notorious issue annoying EGS researchers and engineers [7,15,42]. From the *x*-velocity distribution, shown in Fig. 3, we see an obvious preferential flow exists in the reservoir of the doublet EGS, i.e. case 1. The fluid prefers to flow in a narrow-*z* region centering about the mid-*z* *xy*-plane.

Fig. 4 shows the temperature of rock in the reservoir at four time instants. Upon the EGS operation, the injected cold fluid quickly cools down the rock mass adjoining to the injection well borehole and a low rock temperature region forms therein. As the heat extraction process progresses, the low-temperature region gradually expands.

The production temperature as a function of EGS operation time is displayed in Fig. 5. If the fluid can be fully heated-up by the rock, the production temperature is around 460 K, which is the initial average rock temperature in the reservoir. Once the low rock temperature region expands too close to the production well, i.e. at about 8 years into the EGS operation, the fluid does not have sufficient time to extract heat from the rock mass in the reservoir and the production temperature begins to decrease. From Fig. 5 we determine as well the lifetime of this EGS is 19.6 years, i.e. $\tau = 19.6$ years.

We calculated the heat extraction ratio, $\gamma_L(t)$ and $\gamma(t)$. Fig. 6 depicts the calculated $\gamma_L(\tau)$ results. At the end of EGS operation (time $= \tau$), a large portion of heat stored in the reservoir has not been extracted. From the overall heat extraction ratio curve as a function of EGS operation time, $\gamma(t)$, which has been already depicted in Fig. 5, we find the overall heat extraction ratio at the

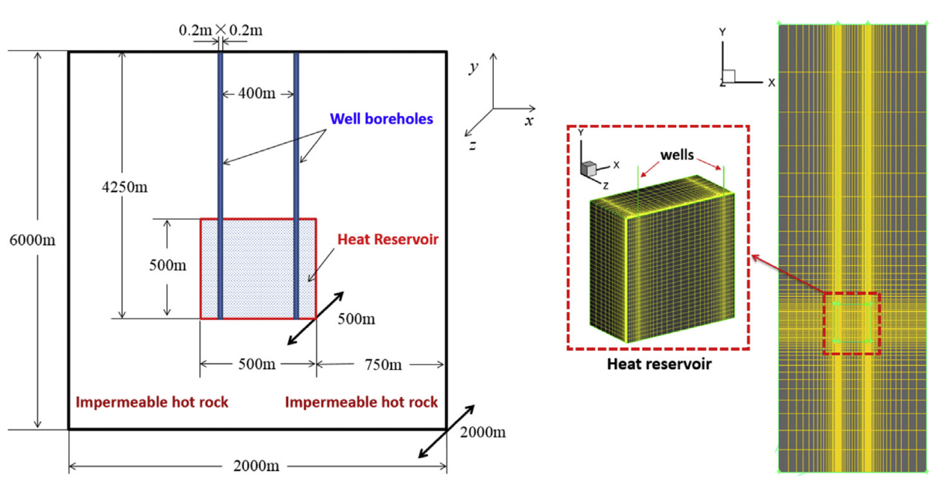

Fig. 1. Geometry (including geometrical dimensions) and mesh of the doublet well EGS.

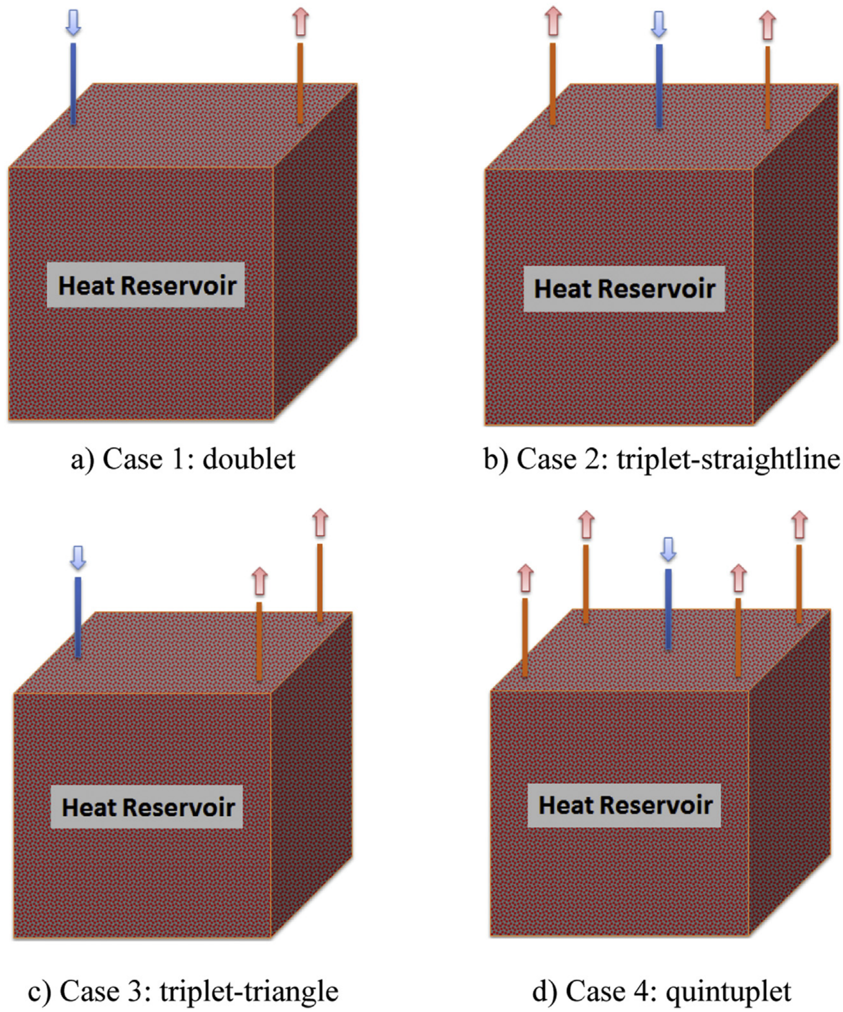

Fig. 2. Schematic of the four well layouts considered.

end of EGS operation, i.e. $\gamma(\tau)$, is only about 0.26. That is to say, about 74% of the total heat stored in the heat reservoir is not mined out.

The preferential flow makes most of the fluid has limited residence time in the reservoir and a large portion of rock mass has little chance to access the heat transmission fluid. The occurrence of preferential flow deteriorates the heat extraction performance and leads to a premature EGS operation.

During EGS operation, the rock mass in the reservoir is cooled by the heat transmission fluid, and a temperature difference is thus formed between the rock matrix in the porous reservoir and the rock enclosing the reservoir. Heat is then conducted from the surrounding impermeable rocks to the reservoir. This thermal compensation action is illustrated in Fig. 7. We see strong thermal compensation action in the vicinity region of the injection well, where the rock mass has been sufficiently cooled down by the injected fluid. We quantify this thermal compensation effect on EGS heat extraction process by the parameter $\beta(t)$, defined by Eq. (7). It is calculated that at the time instant τ (i.e. 19.6 years), β amounts to be 6.3%, meaning accumulatively, about 6.3% of the heat extracted by the outflow fluid has come originally from the rock mass enclosing the reservoir.

Table 2
Cases studied.

Case#	Well layout	Mass flow rate Q (kg/s)	Single-well production Q_s (kg/s)
1	Doublet	50	50
2	Triplet-straightline	50	25
3	Triplet-triangle	50	25
4	Quintuplet	50	12.5

3.2. Well layout effects

During design and practical development of EGS, enhancing subsurface inter-well connectivity and alleviating preferential flow in the reservoir are two important and seemingly conflicting measures that deserve full consideration for achieving better EGS performance. Current reservoir stimulation technologies have not yet reached that high level that can create a reservoir of desired fracture networks with ease [43–45]. The strategy of arranging more than one production well can probably give consideration to both measures aforementioned and has been implemented in a few EGS power stations [5–7]. How does the well layout affect the EGS heat extraction performance and what are the underlying fundamentals? We attempt to answer these questions in the following paragraphs.

Results of fluid flow field in the reservoir for cases 2, 3, and 4 are shown in Fig. 8. The fluid flow pattern in the reservoir is largely

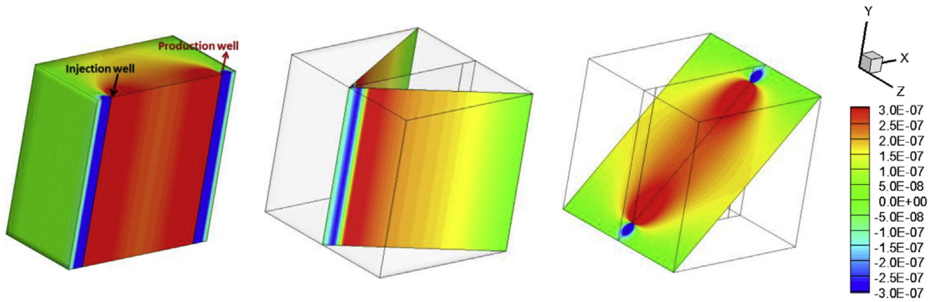

Fig. 3. *x*-Velocity (m/s) distribution in the heat reservoir of the doublet well EGS (case 1). Left: 3D distribution in half of the reservoir geometry; middle: contour plots on two representative planes; right; contour plot on a diagonal plane.

influenced by the well layout. Compared with the corresponding results for case 1 (see Fig. 3), the triplet-straightline well layout (case 2) evidently aggravates the preferential flow and makes the fluid flow being more confined in a narrower-*z* region centering about the mid-*z* *xy*-plane; the triplet-triangle (case 3) and quintuplet (case 4) EGSs both show evident improvement at the fluid flow distribution in the reservoir, in particular for the triplet-triangle well EGS (case 3), the fluid flow distributes quite uniformly in the reservoir.

Fig. 9 presents the production temperature as a function of the EGS operation time for all the four cases. The curves differ from each other mainly at the time duration that the production temperature retains at the maximum production temperature, i.e. about 460 K. Case 3 shows the longest time duration, case 4 the second longest, case 1 the third, and case 2 the shortest. As mentioned in Section 3.1 in relation with Fig. 5, the decrease of production temperature is caused by the injected cold fluid breaks through the reservoir and does not have enough time to extract heat from the rock mass. Therefore, the fluid flow pattern in the reservoir dictates the evolution of production temperature. More uniform flow distribution or less preferential flow in the reservoir leads to better EGS performance. It is easy to determine from Fig. 9 that the EGS lifetimes of the four cases, cases 1, 2, 3, and 4, are 19.6, 9.8, 29.8, and 26.9 years, respectively.

Results shown in Fig. 9 indicate that an EGS of triplet well layout perform better than an EGS of doublet well layout only if the triplet well layout has been properly designed, and an EGS of quintuplet well layout may even perform worse than an EGS of triplet well layout. We further deduce from the calculated results that simply drilling more wells does not surely enhance the EGS performance

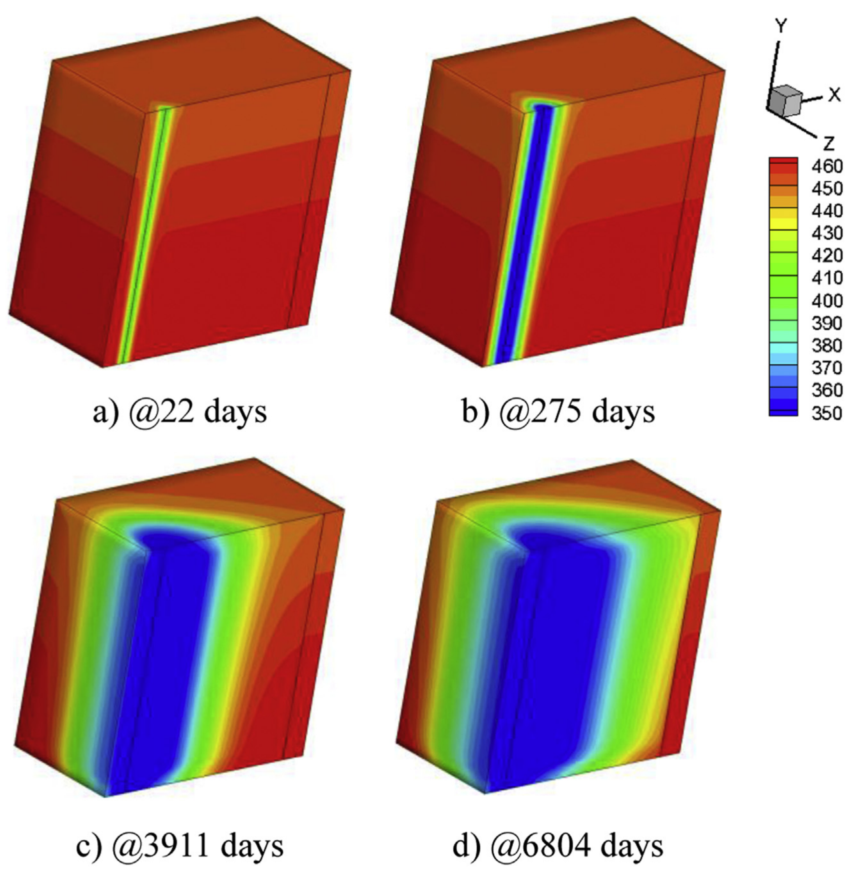

Fig. 4. Temperature (K) of rock in the heat reservoir of the doublet well EGS (case 1).

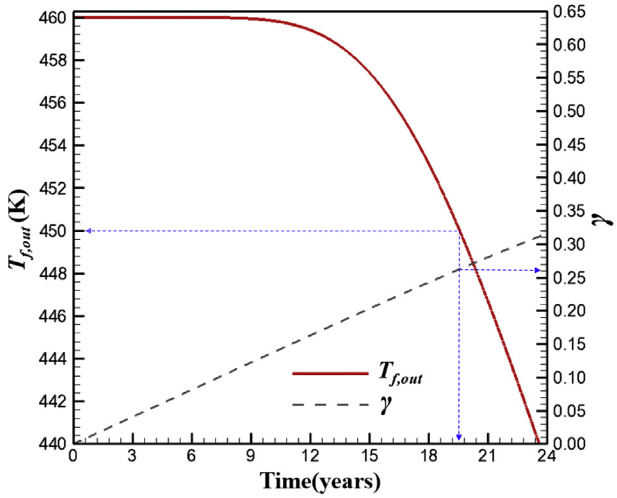

Fig. 5. Production temperature and heat extraction ratio curves for the doublet well EGS (case 1).

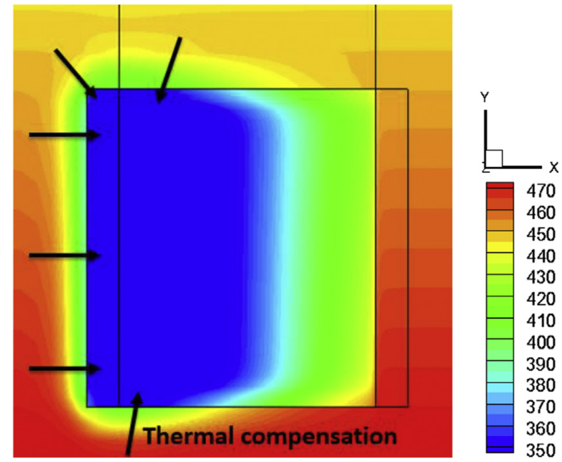

Fig. 7. Rock temperature (K) on the central *xy*-plane at the end of the EGS operation for case 1.

as the well layout may play a more determinant role, not even mentioning drilling more wells may significantly increase the initial investment of EGS plants.

We calculate the local heat extraction ratio in the reservoir and present its distribution on a representative plane of the reservoir at the end of EGS operation in Fig. 10 for all the four cases. Specially, we draw additionally iso-value surfaces with $\gamma_L(\tau) = 0.4$ in this figure. These plots clearly show that the heat extraction process of case 3 has been carried out with the best completeness, case 4 the second best, case 1 the third, and case 2 the worst. All the four cases are seen to have some regions with very low local heat extraction ratio. Generally, the low heat extraction ratio regions are close to the production well or wells.

Fig. 11 summarizes the calculated overall heat extraction ratio and thermal compensation proportion at the end of EGS operation, i.e. $\gamma(\tau)$ and $\beta(\tau)$ for all the four cases. It is seen that the final overall heat extraction ratio for the EGSs with different well layouts varies within 0.136–0.397. The EGS of triplet-straightline well layout has the worst heat extraction performance, the doublet well EGS the second worst, the quintuplet well EGS the third worst, and the EGS of triplet-triangle well layout the best. The final thermal compensation proportions are 0.063, 0.020, 0.075, and 0.035 for the doublet well EGS, the EGS of triplet-straightline well layout, the EGS of triplet-triangle well layout, and the quintuplet well EGS, respectively. The doublet well EGS and the EGS of triplet-triangle well layout get relatively larger amount of thermal compensation from the rocks enclosing the reservoir mainly due to the fact that the injection well is located close to the edge of the reservoir. During EGS operation, a low rock temperature region is formed in the vicinity region of the injection well (Refer to Figs. 4, 6 and 10). Positioning the injection well close to the edge of the reservoir thereby facilitates the thermal compensation process (Refer to Fig. 7). The EGS of triplet-triangle well layout gets slightly more thermal compensation than the doublet well EGS as the former has longer lifetime. The same reason leads to the slight difference (0.015) of thermal compensation proportion between the quintuplet well EGS and the EGS of triplet-straightline well layout.

3.3. Design of well layout

From the results detailed in Sections 3.1 and 3.2, we see that multiplet well layout does have positive effects on the heat extraction of EGS if the well layout is properly designed. The analyses in the foregoing sub-sections also indicate that at least two basic principles need to be followed during the design of EGS well layout: 1) longer major flow path; 2) less preferential flow. Fig. 12 illustrates the length of major flow path in reservoirs of EGSs with different well layouts. It is seen that the triplet-straightline well layout simply reduces half of the major flow path of the doublet well EGS, the other two cases both have longer major flow path than the doublet well layout, and the triplet-triangle well layout has the longest flow path. In addition, to maximize the thermal compensation from rocks enclosing the reservoir, the injection well needs to be positioned close to the edge of the reservoir. As the triplet-triangle well layout strictly follows all the principles, it gives the best heat extraction performance.

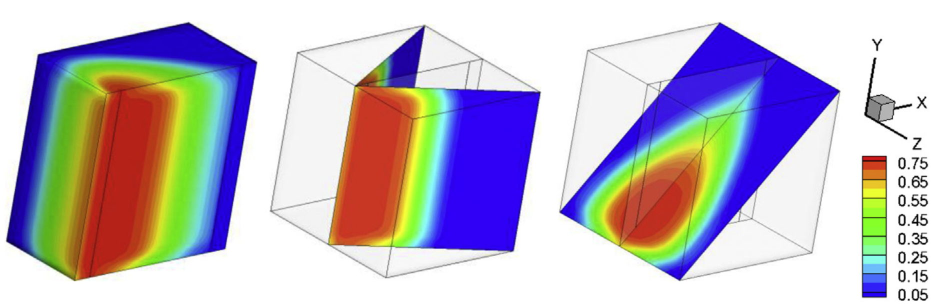

Fig. 6. The final local heat extraction ratio distribution, $\gamma_L(\tau)$, in the heat reservoir of the doublet well EGS (case 1). Left: 3D distribution in half of the reservoir geometry; middle: contour plots on two representative planes; right; contour plot on a diagonal plane.

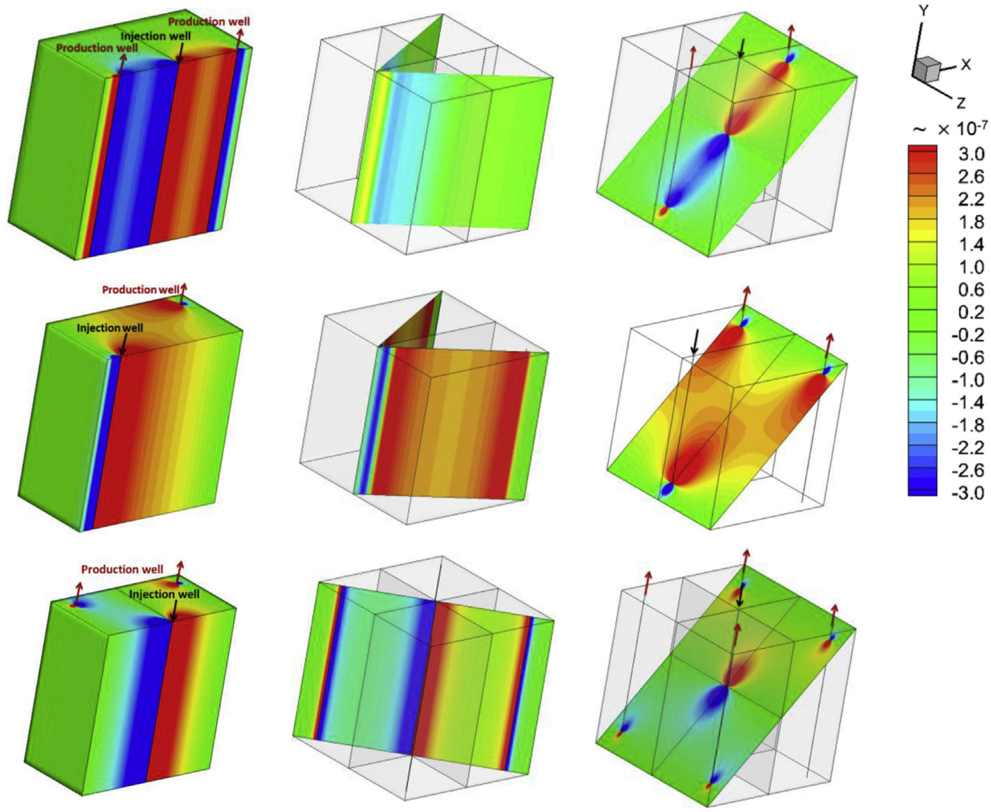

Fig. 8. *x*-Velocity (m/s) distribution in the reservoir for cases 2, 3 and 4. Upmost row: case 2; mid-row: case 3; bottom row: case 4. Left column: 3D distribution in half of the reservoir geometry; middle column: contour plots on two representative planes; right column; contour plot on a diagonal plane.

Accordingly, we further design a quartuplet well layout (schematic displayed in Fig. 13) and simulate the long-term operation of this quartuplet well EGS. Its lifetime is calculated to be 30.6 years and the final overall heat extraction ratio is 0.408. Both are a little better than those of case 3, validating the basic principles we proposed for the design of EGS well layout. It is worth pointing out that the improvement at the EGS heat extraction performance is not significant compared to the EGS of triplet-triangle well layout, indicating the triplet-triangle well layout is already a very good well layout design.

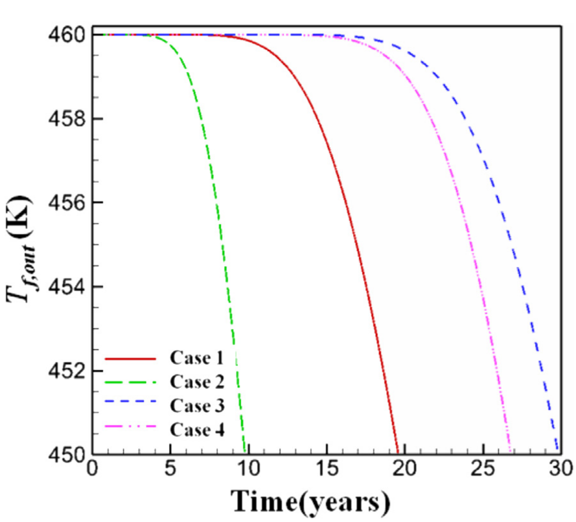

Fig. 9. Evolution of EGS production temperature for all the four cases.

3.4. Estimation of recoverable HDR resource

The HDR heat resource is ubiquitous across the planet. Nevertheless, there are some places, which may be not suitable for EGS construction due to social and/or humanistic factors, such as national parks, recreation areas, urban areas, major highways, utility corridors, and national monuments. Besides, the regions where the geothermal gradient is relatively low, the areas where the underground rock is too stiff to drill, and/or the places where water (i.e. the common heat transmission fluid) is very scarce are all not appropriate choices for EGS construction from a commercial perspective. To estimate the potential of HDR heat resource, all these factors must be taken into account. More importantly, both the fraction of heat that can be extracted from EGS reservoir and the heat-to-electricity conversion coefficient provide the most compelling information for the estimation. A recovery factor of 2%, which may be somewhat conservative, was used to estimate the potential of HDR heat resource in US [1].

Since the total heat reserve in HDR is constant, the heat extraction ratio becomes the most important factor that influences the estimation of EGS potential [46]. Considerable efforts [24–26] have been expended to estimate the HDR heat recovery factor. Sanyal and Butler [24] used a 3-dimensional numerical model and calculated the fraction of HDR heat that could be extracted. They found that the recoverable heat from a minimum 1×10^8 m^3 (approximately 500 × 500 × 500 m dimensions) reservoir volume is within 34%–47% of the total heat stored, and they asserted that this recovery factor is independent of well layout, fracture spacing, and reservoir permeability, as long as the reservoir volume exceeds 1×10^8 m^3. Grant and Garg [25] expressed their doubts on Sanyal and Butler's results as the used model by Sanyal and Butler

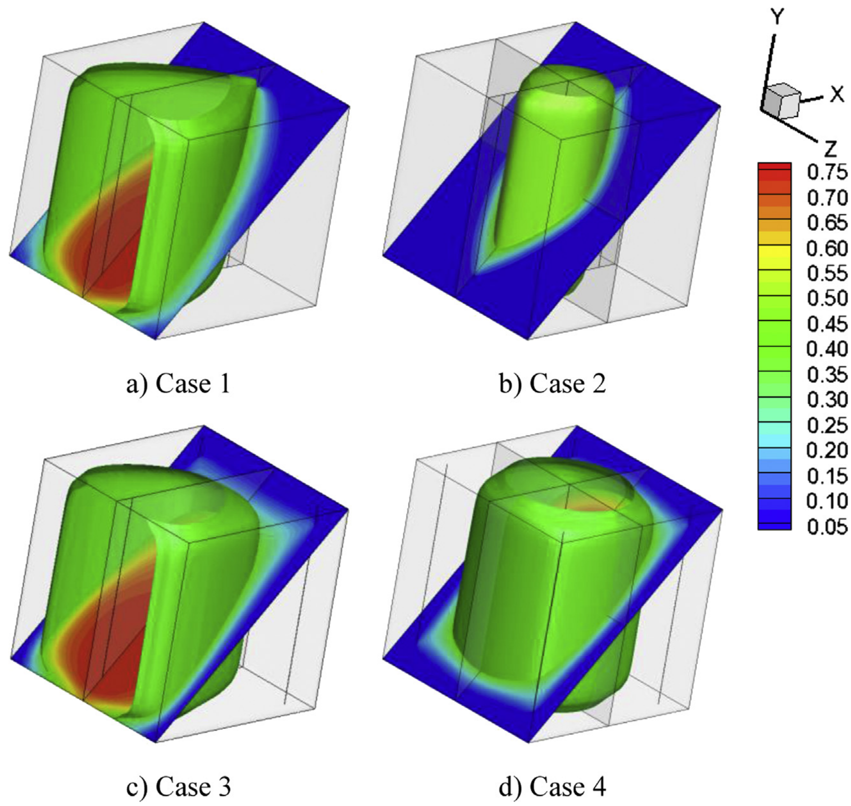

Fig. 10. The final local heat extraction ratio distribution in the reservoir and an iso-surface with $\gamma_L(\tau) = 0.4$ for all the four cases.

encompassed too many simplifications. Williams [26] also suggested a much different HDR heat recovery factor, less than 0.1. To date, there are yet no field test data on the long-term heat extraction process of EGS, which makes validation and calibration of the numerical results extremely difficult. Nevertheless, numerical simulation based on rational simplification models may still be the most effective method for the estimation of HDR recoverable heat.

The present work takes the reservoir as a homogeneous porous medium and the overall heat extraction ratio, defined by Eq. (6), at the end of EGS operation, i.e. $\gamma(\tau)$, is actually the HDR heat recovery factor. Besides the 4 cases listed in Table 2, we simulated 18 cases more. The calculated recovery factors, summarized in Table 3, are found to be within a range of 13%–49%, strongly dependent on the well layout of EGS, whereas relatively less dependent on the other parameters examined. If considering a 10% heat-to-electricity conversion efficiency [47] and an additional reduction factor of 0.95 as some places may be not suitable for constructing EGS plants, we estimate the potential of HDR heat for electricity-generation is only about 1.2%–4.9% of the total heat storage.

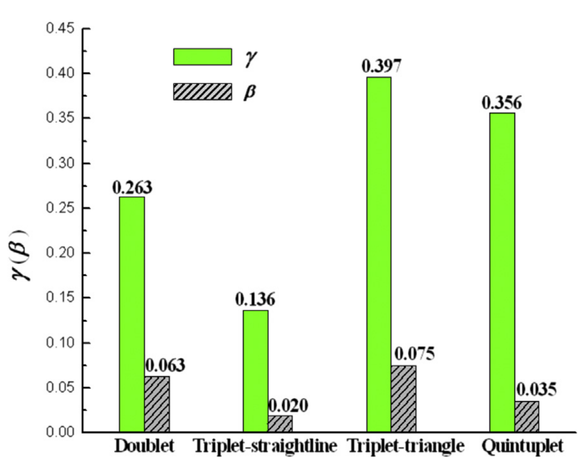

Fig. 11. Overall heat extraction ratio and thermal compensation proportion at the end of EGS operation for all the four cases.

4. Confidence estimation of model results

To establish sufficient confidence of model results, we do additionally the following three aspects of model validation work. First, we evaluate numerical errors based on the Richardson extrapolation technique [48]. For the case of quintuplet well layout (i.e. case 4), three calculations with different numerical mesh systems were performed. The three mesh systems have numerical elements (N_e): 269,080, 362,880 and 1,164,870, respectively. Assuming the obtained heat extraction ratio $\gamma(\tau)$ to be linearly dependent on the parameter, $1/(N_e)$, we determine the accurate value of $\gamma(\tau)$, taken when N_e equals infinite, is 0.3688. The mesh system employed in the present work, which has 269,080 numerical elements, gives $\gamma(\tau) = 0.356$ (see in Fig. 11), deviating the extrapolated accurate value by 3.47% only.

Second, we compare the present model results with some published results. Aimed to explore the involved multi-disciplinary transport in EGS subsurface geometry during heat extraction, numerous numerical models [19,21,49–54] have been developed. Despite different methods used and different geological conditions considered, all these published works confirmed that the fluid flow distribution in heat reservoir is an important factor dictating the heat extraction performance of EGS. Moreover, the obtained curves (see e.g. Fig. 5 in Ref. [19], Figs. 9 and 10 in

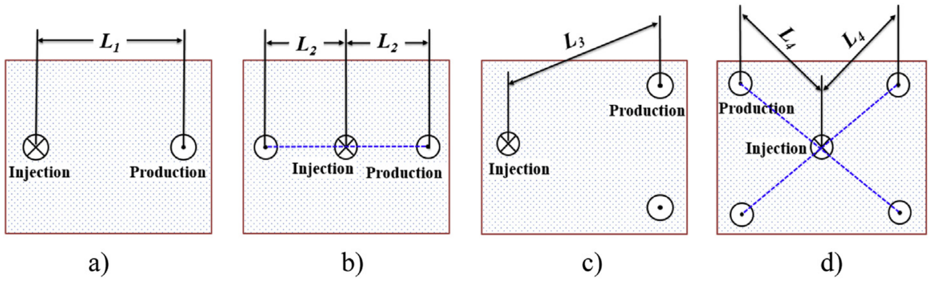

Fig. 12. Length of major flow path, a) the doublet well layout, b) triplet-straightline well layout, c) triplet-triangle well layout, and d) quintuplet well layout. $L_2 = 0.5\ L_1$, $L_3 = 1.12\ L_1$, $L_4 = 0.71\ L_1$.

Ref. [49], Fig. 5 in Ref. [50], Fig. 11 in Ref. [51], and Fig. 2 in Ref. [53]) of production temperature versus EGS operation time are qualitatively similar to the results displayed in Figs. 5 and 9 of the present work.

Third, we compare the model predictions with measured data from EGS field tests. Though numerous projects aimed to develop EGS pilot plants have been and are still being conducted around the world, there are generally no measured data about long-term (i.e. 10 or even 20 years) fluid circulation operation [55]. Numerical model results including the results obtained in the present work show that if there is no severe preferential flow forming in the reservoir and the well borehole casing is well insulated to avoid excessive heat loss, the production temperature will remain steadily at a high level for years. Several mini EGS pilot plants have preliminarily confirmed this [55]. It is expected that more and more EGS field test results will be gradually unveiled in the future, which makes further validation of numerical models become feasible.

5. Conclusions

We assumed the EGS subsurface heat reservoir as homogeneous porous medium and carried out a series of numerical simulations to evaluate and analyze the effects of well layout on EGS heat extraction performance. For the four cases of distinct well layouts considered, the triplet-triangle well EGS shows the best heat extraction performance. A detailed analysis to the simulation results revealed the underlying mechanisms. The triplet-triangle well layout effectively restrains preferential flow in the reservoir and at the same time keeps the major flow path sufficiently long. The thermal compensation from un-fractured rocks surrounding the reservoir contributes some to the heating of the circulating fluid; about a few percent of the cumulative heat extraction amount can come from the heat stored in these rocks. Moreover, positioning the injection well close to the edge of the reservoir effectively facilitates the thermal compensation process.

Specially, for the EGS considered, which is of a $500 \times 500 \times 500$ m homogeneously fractured reservoir, the triplet-triangle well layout may be the best choice for heat extraction, since even with an optimized quartuplet well layout, little improvement at the heat extraction performance can be achieved. The HDR heat recovery factors calculated from 22 cases are found to be within 13%–49%, which show strong dependence on the well layout, whereas relatively slight dependence on the parameters like the reservoir permeability, the geothermal gradient, the fluid flow rate, and the fluid injection temperature. Accordingly, we estimate the potential of HDR heat for electricity-generation is about 4.9% maximized.

For real heterogeneous heat reservoirs, the obtained heat recovery factors may be exaggerated to some extent and the optimized well layout may be significantly different from the triplet-triangle well layout or quartuplet well layout proposed in the present work. Nevertheless, the proposed principles: longer major flow path, less preferential flow, and positioning the injection well

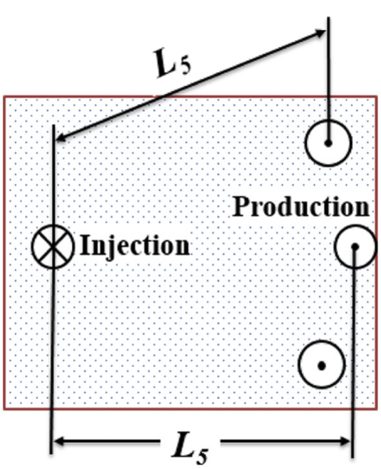

Fig. 13. Schematic of the optimized quartuplet well layout, $L_5 = L_3 = 1.12\ L_1$.

Table 3
Cases considered for the estimation of HDR recoverable heat and the obtained results.

Case#	Well layout	K (m^2)	∇T (K/100 m)	Q (kg/s)	$T_{f,in}$ (K)	τ (year)	γ (%)	$\beta(\tau)$ (%)
1	Doublet	10^{-14}	4	50	343	19.6	26.3	6.3
2	Triplet-straightline	10^{-14}	4	50	343	9.8	13.6	1.96
3	Triplet-triangle	10^{-14}	4	50	343	29.8	39.7	7.50
4	Quintuplet	10^{-14}	4	50	343	26.9	35.6	3.5
5	Doublet	10^{-14}	4	150	343	6.34	26.0	2.06
6	Doublet	10^{-10}	4	150	343	6.7	26.1	2.12
7	Doublet	10^{-12}	4	150	343	6.34	26.0	2.06
8	Doublet	10^{-16}	4	150	343	6.34	26.0	2.06
9	Triplet-straightline	10^{-14}	4	150	343	3.11	12.44	0.87
10	Triplet-triangle	10^{-14}	4	150	343	9.8	38.5	3.78
11	Quintuplet	10^{-14}	4	150	343	8.58	35.2	1.73
12	Triplet-straightline	10^{-14}	4	100	343	4.76	12.83	1.20
13	Triplet-triangle	10^{-14}	4	100	343	14.85	48.9	4.94
14	Quintuplet	10^{-14}	4	200	343	6.38	33.33	1.39
15	Doublet	10^{-14}	4	50	300	18.3	34.65	5.20
16	Triplet-straightline	10^{-14}	4	50	300	8.95	15.79	1.86
17	Triplet-triangle	10^{-14}	4	50	300	28.35	48.55	7.32
18	Quintuplet	10^{-14}	4	50	300	24.24	44.32	3.40
19	Doublet	10^{-14}	5	50	343	18.33	25.9	5.2
20	Triplet-straightline	10^{-14}	5	50	343	8.99	13.2	1.8
21	Triplet-triangle	10^{-14}	5	50	343	28.43	38.6	6.7%
22	Quintuplet	10^{-14}	5	50	343	24.32	34.3	3.2%

as close as possible to the edge of the reservoir, for the design of advanced well layout should be still effective. It is worth pointing out as well that better heat extraction performance of EGS may be achieved by other measures, for instance, drilling directional or horizontal wells, other than designing multi-well heat extraction mode of particular interest in the present work.

Acknowledgments

Financial support received from the China National "863" Project (2012AA052802), the CAS "100 talents" Program (FJ), and the China National Science Foundation (51206174) is gratefully acknowledged.

Nomenclature

a	specific surface area of aperture network (m^2/m^3)
c_p	heat capacity (J/kg/K)
$\mathbf{g}$	acceleration of gravity (m/s^2)
h	convective heat transfer coefficient ($W/m^2/K$)
k	thermal conductivity (W/m/K)
k_s^{eff}	effective thermal conductivity of rock (W/m/K)
k_f^{eff}	effective thermal conductivity of heat transmission fluid (W/m/K)
K	reservoir permeability (m^2)
L	distance from injection well to production well (m)
L_1	distance from injection well to production well of case 1 (m)
L_2	distance from injection well to production well of case 2 (m)
L_3	distance from injection well to production well of case 3 (m)
L_4	distance from injection well to production well of case 4 (m)
L_5	distance from injection well to production well of the quartuplet EGS (m)
N_e	number of numerical elements (−)
p	pressure (Pa)
Q	mass flow rate of heat transmission fluid (kg/s)
Q_s	single-well production of heat transmission fluid (kg/s)
t	time (s)
t'	time (s)
T	temperature (K)
T_f	liquid temperature (K)
$T_{f,a}$	abandonment temperature (K)
$T_{f,in}$	injection temperature (K)
T_o	ground surface temperature (K)
$T_{f,out}$	production temperature (K)
T_s	rock temperature (K)
$T_{s,i}$	initial rock temperature (K)
$\mathbf{u}$	velocity vector (m/s)
v	volume (m^3)
V_R	reservoir volume (m^3)
V_S	volume of rock surrounding the reservoir (m^3)
x	horizontal axis in Cartesian coordinates
y	vertical axis in Cartesian coordinates
z	horizontal axis in Cartesian coordinates

Greek symbols

ρ	density (kg/m^3)
ε	porosity (−)
μ	viscosity (Pa s)
τ	EGS lifetime (years)
β	proportion of thermal compensation
γ	heat extraction ratio
γ_L	local heat extraction ratio
θ	time (s)
∇T	geothermal gradient (K/100 m)

Subscripts/superscripts

eff	effective
i	initial
L	local
f	fluid
s	solid or rock or single well

References

[1] Tester JW, Anderson BJ, Batchelor AS, Blackwell DD, DiPippo R, Drake EM, et al. The future of geothermal energy. Massachusetts Institute of Technology; 2006. p. 358.

[2] Wang GL, Li KW, Lin WJ, Lin LJ, Liu ZM, Zhang W, et al. Assessment of geothermal resources in China. In: 38th Workshop on Geotherm Reserv Eng. Stanford, CA: Stanford Univ.; 2013.

[3] Lacirignola M, Blanc I. Environmental analysis of practical design options for enhanced geothermal systems (EGS) through life-cycle assessment. Renew Energy 2013;50:901–14.

[4] U.S. Department of Energy. An evaluation of enhanced geothermal systems technology; 2008.

[5] Brown DW, Duchane DV. Scientific progress on the Fenton Hill HDR project since 1983. Geothermics 1999;28:591–601.

[6] Genter A, Evans K, Cuenot N, Daniel Fritsch, Sanjuan B. Contribution of the exploration of deep crystalline fractured reservoir of Soultz to the knowledge of enhanced geothermal systems (EGS). C R Geosci 2010;342:502–16.

[7] Tenma N, Yamaguchi T, Zyvoloski G. The Hijiori hot dry rock test site, Japan: evaluation and optimization of heat extraction from a two-layered reservoir. Geothermics 2008;37:19–52.

[8] Giroud N, Vuataz FD, Schill E, (Centre for Hydrogeology and Geothermics, University of Neuchâtel). Geothermal reservoir of the EGS pilot plant at Soultz-sous-Forêts (France): monitoring of the exploitation and prediction of its behavior. Final report 2009 – 2012. Deep Heat Mining Association; 2012 Nov.. Contract No.: 500'073-01/Project No.: 500'073.

[9] Matek B. 2013 Annual US geothermal power production and development report. Pennsylvania Avenue SE, Washington, D.C.: Geothermal Energy Association; 2013.

[10] Polsky Y, Capuano L, Finger J, Huh M, Knudsen S, Mansure AJ, et al., (Sandia National Laboratories, Albuquerque, New Mexico and Livermore, California). Enhanced geothermal systems (EGS) well construction technology evaluation report. United States Department of Energy (US); 2008 Dec.. Contract No.: DE-AC04-94AL85000.

[11] Barbier E. Geothermal energy technology and current status: an overview. Renew Sustain Energy Rev 2002;6:3–65.

[12] Wang F, Ren TX, Hungerford F, Tu S, Aziz N. Advanced directional drilling technology for gas drainage and exploration in Australian coal mines. Procedia Eng 2011;26:25–36.

[13] Aadnoy BS, Looyeh R. Petroleum rock mechanics: drilling operations and well design. 1st ed. Oxford: Gulf Professional Publishing; 2011.

[14] Elders WA, Friðleifsson GÓ, Albertsson A. Drilling into magma and the implications of the Iceland Deep Drilling Project (IDDP) for high-temperature geothermal systems worldwide. Geothermics 2014;49:111–8.

[15] Vogt C, Kosack C, Marquart G. Stochastic inversion of the tracer experiment of the enhanced geothermal system demonstration reservoir in Soultz-sous-Forêts—revealing pathways and estimating permeability distribution. Geothermics 2012;42:1–12.

[16] Kathryn Dee Co C. Characterization of geothermal feedzones and interwell connectivity [dissertation]. Stanford: Stanford University; 2012.

[17] Karrech A. Non-equilibrium thermodynamics for fully coupled thermal hydraulic mechanical chemical processes. J Mech Phys Solids 2013;61:819–37.

[18] Taron J, Elsworth D. Thermal–hydrologic–mechanical–chemical processes in the evolution of engineered geothermal reservoirs. Int J Rock Mech Min Sci 2009;46:855–64.

[19] Finsterle S, Zhang Y, Pan L, Dobson P, Oglesby K. Microhole arrays for improved heat mining from enhanced geothermal systems. Geothermics 2013;47:104–15.

[20] Neuville A, Toussaint R, Schmittbuhl J. Fracture roughness and thermal exchange: a case study at Soultz-sous-Forêts. C R Geosci 2010;342:616–25.

[21] Bataillé A, Genthon P, Rabinowicz M, Fritz B. Modeling the coupling between free and forced convection in a vertical permeable slot: implications for the heat production of an enhanced geothermal system. Geothermics 2006;35(5):654–82.

[22] Jiang FM, Chen JL, Huang WB, Luo L. A three-dimensional transient model for EGS subsurface thermo-hydraulic process. Energy 2014;72:300–10.

[23] Jiang FM, Luo L, Chen JL. A novel three-dimensional transient model for subsurface heat exchange in enhanced geothermal systems. Int Commun Heat Mass Transf 2013;41:57–62.

[24] Sanyal SK, Butler SJ. An analysis of power generation prospects from enhanced geothermal systems. In: Proceedings World Geothermal Congress; 2005 Apr 24–29; Antalya, Turkey; 2005.
[25] Grant MA, Garg SK. Recovery factor for EGS. In: 37th Workshop on Geotherm Reserv Eng. Stanford, CA: Stanford Univ.; 2012.
[26] Williams CF. Thermal energy recovery from enhanced geothermal systems – evaluating the potential from deep, high-temperature resources. In: 35th Workshop on Geotherm Reserv Eng. Stanford, CA: Stanford Univ.; 2010.
[27] Petty S, Porro G. Updated US geothermal supply characterization. In: 32nd Workshop on Geotherm Reserv Eng. Stanford, CA: Stanford Univ.; 2007.
[28] Latham JP, Xiang J, Belayneh M, Nick HM, Tsang CF, Blunt MJ. Modelling stress-dependent permeability in fractured rock including effects of propagating and bending fractures. Int J Rock Mech Min Sci 2012;57:100–12.
[29] Portier S, Vuataz FD, Nami P, Sanjuan B, Gérard A. Chemical stimulation techniques for geothermal wells: experiments on the three-well EGS system at Soultz-sous-Forêts, France. Geothermics 2009;38:349–59.
[30] Moeck I, Kwiatek G, Zimmermann G. Slip tendency analysis, fault reactivation potential and induced seismicity in a deep geothermal reservoir. J Struct Geol 2009;31:1174–82.
[31] Simone SD, Vilarrasa V, Carrera J, Alcolea A, Meier P. Thermal coupling may control mechanical stability of geothermal reservoirs during cold water injection. J Phys Chem Earth 2013;64:117–26.
[32] Ghassemi A, Zhou X. A three-dimensional thermo-poroelastic model for fracture response to injection/extraction in enhanced geothermal systems. Geothermics 2011;40:39–49.
[33] Grant MA, Clearwater J, Quinão J, Bixley PF, Brun ML. Thermal stimulation of geothermal wells: a review of field data. In: 38th Workshop on Geotherm Reserv Eng. Stanford, CA: Stanford Univ.; 2013.
[34] Radilla G, Sausse J, Sanjuan B, Fourar M. Interpreting tracer tests in the enhanced geothermal system (EGS) of Soultz-sous-Forêts using the equivalent stratified medium approach. Geothermics 2012;44:43–51.
[35] Crandall D, Siriwardane H, Bromhal G. Modeling fluids and fractures in geothermal systems. In: Proceedings of the ASME 2011 5th International Conference on Energy Sustainability; 2011 Aug 7-10; Washington, DC, USA; 2011. ES2011-54337.
[36] Manga M, Beresnev I, Brodsky EE, Elkhoury JE, Elsworth D, Ingebritsen SE, et al. Changes in permeability caused by transient stresses: field observations, experiments, and mechanisms. Rev Geophys 2012;50:1–24.
[37] Brown DW. A hot dry rock geothermal energy concept utilizing supercritical CO_2 instead of water. In: 25th Workshop on Geotherm Reserv Eng. Stanford, CA: Stanford Univ.; 2000.
[38] Häring MO, Schanz U, Ladner F, Dyer BC. Characterisation of the Basel 1 enhanced geothermal system. Geothermics 2008;37:469–95.
[39] Tezuka K, Niitsuma H. Stress estimated using microseismic clusters and its relationship to the fracture system of the Hijiori hot dry rock reservoir. Eng Geol 2000;56:47–62.
[40] Sanjuan B, Pinault JL, Peter Rose, Gérard A, Brach M, Braibant G, et al. Tracer testing of the geothermal heat exchanger at Soultz-sous-Forêts (France) between 2000 and 2005. Geothermics 2006;35:622–53.
[41] Ledésert B, Hebert R, Genter A, Bartier D, Clauer N, Grall C. Fractures, hydrothermal alterations and permeability in the Soultz enhanced geothermal system. C R Geosci 2010;342:607–15.
[42] Parker R. The Rosemanowes HDR Project 1983–1991. Geothermics 1999;28:603–15.
[43] Economides MJ, Nolte KG, Ahmed U. Reservoir stimulation. 3rd ed. New York: Wiley; 2000.
[44] Evans KF, Genter A, Sausse J. Permeability creation and damage due to massive fluid injections into granite at 3.5 km at Soultz: 1. Borehole observations. J Geophys Res 2005;110(B4):B04203.
[45] Zimmermann G, Reinicke A. Hydraulic stimulation of a deep sandstone reservoir to develop an enhanced geothermal system: laboratory and field experiments. Geothermics 2010;39:70–7.
[46] Chamorro CR, García-Cuesta JL, Mondéjar ME, Linares MM. An estimation of the enhanced geothermal systems potential for the Iberian Peninsula. Renew Energy 2014;66:1–14.
[47] Yari M. Exergetic analysis of various types of geothermal power plants. Renew Energy 2010;35:112–21.
[48] Shyy W, Garbey M, Appukuttan A, Wu J. Evaluation of Richardson extrapolation in computational fluid dynamics. Numer Heat Transf Part B Fundam 2002;41(2):139–64.
[49] Blöcher MG, Zimmermann G, Moeck I, Brandt W, Hassanzadegan A, Magri F. 3D numerical modeling of hydrothermal processes during the lifetime of a deep geothermal reservoir. Geofluids 2010;10(3):406–21.
[50] Shaik AR, Rahman SS, Tran NH, Tran T. Numerical simulation of fluid-rock coupling heat transfer in naturally fractured geothermal system. Appl Therm Eng 2011;31(10):1600–6.
[51] Fox DB, Sutter D, Beckers KF, Lukawski MZ, Koch DL, Anderson BJ, et al. Sustainable heat farming: modeling extraction and recovery in discretely fractured geothermal reservoirs. Geothermics 2013;46:42–54.
[52] Watanabe N, Wang W, McDermott CI, Taniguchi T, Kolditz O. Uncertainty analysis of thermo-hydro-mechanical coupled processes in heterogeneous porous media. Comput Mech 2010;45(4):263–80.
[53] Brown D, DuTeaux R, Kruger P, Swenson D, Yamaguchi T. Fluid circulation and heat extraction from engineered geothermal reservoirs. Geothermics 1999;28(4):553–72.
[54] Taron J, Elsworth D. Coupled mechanical and chemical processes in engineered geothermal reservoirs with dynamic permeability. Int J Rock Mech Min Sci 2010;47(8):1339–48.
[55] Breede K, Dzebisashvili K, Liu X, Falcone G. A systematic review of enhanced (or engineered) geothermal systems: past, present and future. Geotherm Energy 2013;1(1):1–27.